

# Gravitational Mesoscopic Constraints in Cosmological Dark Matter Halos

Christine C. Dantas

*Instituto de Aeronáutica e Espaço (IAE/CTA),  
Pça. Mal. Eduardo Gomes, 50,  
CEP 12.228-904 - Vila das Acácias  
São José dos Campos - SP - Brazil  
ccdantas@iae.cta.br*

and

Fernando M. Ramos

*Laboratório Associado de Computação e Matemática Aplicada,  
INPE/MCT, CP 515,  
S. J. dos Campos, 12201-970 SP, Brazil.  
fernando@lac.inpe.br*

## ABSTRACT

We present an analysis of the behaviour of the ‘coarse-grained’ (‘mesoscopic’) rank partitioning of the mean energy of collections of particles composing virialized dark matter halos in a  $\Lambda$ -CDM cosmological simulation. We find evidence that rank preservation depends on halo mass, in the sense that more massive halos show more rank preservation than less massive ones. We find that the most massive halos obey Arnold’s theorem (on the ordering of the characteristic frequencies of the system) more frequently than less massive halos. This method may be useful to evaluate the coarse-graining level (minimum number of particles per energy cell) necessary to reasonably measure signatures of ‘mesoscopic’ rank orderings in a gravitational system.

*Subject headings:* dark matter halos, fundamental plane of elliptical galaxies, scaling relations, n-body simulations

## 1. Introduction

Dissipationless N-body simulations of stellar systems indicate that scaling relations such as the so-called ‘Fundamental Plane’ (hereon, FP), that is, the systematic deviation from the expectations of the virial theorem applied to these systems (e.g., Djorgovski & Davis 1987; Dressler et al. 1987; Pahre 1998; Hjorth & Madsen 1995; Bekki 1998; Djorgovski 1988, 1993; Dantas et al.

2000), could be reproduced from the final products of hierarchical merging of galactic model progenitors (Capelato et al. 1995). However, not all evolutionary conditions lead to FP-like relations: simple gravitational collapses do not. That is, objects resulted from mergers form a slightly non-homologous family (and a FP-like relation), whereas collapses are homologous among themselves (and show no deviation from the virial expectations; see Dantas et al. 2002).

At the same time, Kandrup and collaborators (Kandrup et al. 1993) argued on the existence of ‘mesoscopic constraints’ of pure gravitational origin in systems relaxing towards virialization (hereon, the ‘Kandrup Effect’). These constraints were inferred from the general preservation of the ‘coarse-grained’ partitioning of the ranked energy distribution of particles, and seemed to regulate somehow the gravitational evolution of these galaxy models towards equilibrium. These constraints were also indirectly shown to be partially ‘broken’ (violated) in mergers and fully operative in collapses (Dantas et al. 2003).

The effect of incomplete mixing of phase space in dissipationless gravitational collapses was known already since the decade of 80s (e.g., White 1979; van Albada 1982; May & van Albada 1984; Quinn & Zurek 1988; Zaroubi et al. 1996). The surviving memory of initial conditions in the sense of an almost linear dependence of the final (after the collapse) energies with the initial energies (in cosmological initial conditions) was first demonstrated in (Voglis, Hiotelis & Hoefflich 1991). A more detailed investigation of this effect in N-body systems resulting from cosmological collapses is given in Voglis, Hiotelis & Harsoula (1994).

Such clues lead us to inquire whether the ‘Kandrup Effect’ and the scaling relations of gravitational systems (like the FP) could be deeply related in some way. Here we present a ‘global map’ indicating where mesoscopic constraints could be mostly operative, in a full cosmological simulation. This paper is organized as follows. In Section 2, we study the ‘Kandrup Effect’ in terms of dark matter halos. In Section 3, we investigate the behaviour of halos in terms of Arnold’s theorem on the ordering of characteristic frequencies under the imposition of a linear constraint. In Section 4, we discuss our results.

## 2. Rank Ordering Preservation of Energy Cells in Dark Matter Halos

In the study of Kandrup et al., the distribution of the energy of the particles in systems resulting from collisions and merging of two model galaxies was analysed in detail. They have found that there is a ‘coarse-grained’ sense in which the *ordering* of the mean energy of given collections of particles of the systems is strictly *not violated* through the gravitational evolution of the models towards equilibrium.

The method consists of sorting the particles of a given initial model according to their energies. The models are partitioned into a few, ‘mesoscopic’ (around 5 to 10) bins of equal number of particles and for each of these bins, the mean energy is calculated. Finally, the bins are ranked with the first one initially containing the most bound particles (the most negative mean energy)

whereas the last bin contains the least bounded particles (the least negative mean energy). The mean energies of these same collections of particles are then recalculated for the final model and compared with their initial values. From such an analysis, Kandrup et al. found that the mean energy rank ordering of fixed collections of particles is preserved along the evolution.

Here analyse the ‘Kandrup Effect’ in larger gravitationally-dominated structures, like clusters and superclusters of galaxies (see also Dantas & Ramos 2005). To this end, we have analysed a  $\Lambda$ -CDM N-body simulation output of the VIRGO Consortium. The analysis is identical to that of Dantas et al. (2003), but here the initial condition is the  $z=10$  simulation box, and the final condition, the  $z=0$  box (the boxes have a  $\sim 250$  Mpc comoving size, where each particle has a mass of  $6.86 \times 10^{10} M_\odot$ ). Signs of the ‘Kandrup Effect’ were searched for the 31 most massive halos found in the  $z=0$  box, identified by the use of a simple ‘friends-of-friends’ algorithm (FOF homepage 2005), setting periodic boundary conditions and a searching length of 1 Mpc.

The energy of a particle considered in our work is the mechanical comoving one-particle energy. It was not calculated with respect to the local center of mass of the particular clumps, but with respect to the comoving reference frame (that is, the frame which moves with the cosmological expansion of the simulation box). The comoving energy of a particle  $i$  was calculated classically from:

$$E_i = 1/2mv_i^2 - 1/2 \sum_{j \neq i} Gm^2/|\mathbf{x}_i - \mathbf{x}_j|, \quad (1)$$

with comoving position  $\mathbf{x}_i$  and peculiar velocity  $v_i$ . Units used were Mpc for length, Gyr for time and  $M_\odot$  for mass. The energy associated to the dynamics of expansion of the cosmological box does not enter into the above computations.

At this point we remark that in the present simulation scenario ( $\Lambda$ -CDM), the nonlinear collapse of sub-galactic mass halos are the first expected events after recombination. These small mass units will subsequently cluster together in a hierarchy of larger and larger objects (bottom-up structure formation scenario). This is in contrast to top-down pictures where the formation of very massive objects comes first, as for instance, in the Hot Dark Matter scenario. From the spherical top-hat collapse model, a reasonable estimate for the limit to the redshift at which a given halo becomes virialized or formed ( $z_{vir}$ ) is (Longair 2000):

$$(1 + z_{vir}) \leq 0.47 \left( \frac{v}{100 \text{ km/s}} \right)^2 \left( \frac{M}{10^{12} M_\odot} \right)^{-2/3} (\Omega_0 h^2)^{-1/3}. \quad (2)$$

The less massive halo analysed from the set of 31 objects has a mass of  $10^{13} M_\odot$ . Assuming that its velocity dispersion is of order  $\sim (700 \text{ km/s})^2$  (a typical figure for that mass scale) and the last term of the expression above is of order  $\sim 1$ , we find that  $z_{vir}$  for this halo is approximately  $\leq 4$ . Higher mass halos will have their  $z_{vir}$ ’s even smaller than in above case. For instance, the most massive halo in the simulation has  $M = 10^{14.38} M_\odot$ . Assuming  $v \sim (10^3 \text{ km/s})^2$ , we find  $z_{vir} \leq 0.2$ . Since

all the 31 halos analysed have masses within that range, their condition at  $z = 10$  (the initial dump of the simulation) reasonably represents a linear stage of their evolution. Another way to see this point is that the particle mass of the simulation is  $10^{10.84} M_{\odot}$ . Hence, such a particle is representing a large sub-galactic object, and considering its internal velocity dispersion of  $v \sim (300 \text{ km/s})^2$ , then  $z_{vir} \leq 24$ . Of course, this is the mass resolution of the simulation, it is assumed to already represent a collapsed unit at  $z = 10$ . In other words, that gives an idea of the redshift formation limit for the smallest mass unit resolved in the simulation. Hence, the 31 most massive halos at  $z = 10$  (the first redshift dump available from the simulation) are safely in their linear phases of evolution, so that the comparison of the ‘Kandrup Effect’ seems quite satisfactory to be performed in reasonably equal grounds for all 31 halos.

We have defined a ‘violation’ parameter rate,  $\theta$ , which measures *the degree of rank ordering violation of the mean energy of 10 fixed collections of particles*, compared at  $z = 10$  and  $z = 0$ , so that if  $\theta \rightarrow 0$ , we retrieve the ‘Kandrup Effect’ (no energy rank ordering violation), whereas  $\theta \rightarrow 1$  means that all energy bins presented ordering violation. Notice that the  $\theta$  parameter “penalizes” cases where there is a significant relative change in energy cell position (in the sense of ordering). For example, if only the 10th energy cell crosses all the other 9 cells, and all these 9 cells keep their ordering unaltered, the  $\theta$  parameter in this case is *not* assigned 0.1 (meaning that only one energy cell, out of 10, crosses some other cell - whatever how many places in ordering), but in fact our criteria assigns  $\theta = 1.0$ , meaning that *all* cells are relatively crossed in this case. So the  $\theta$  parameter, although not a weighted parameter, measures in fact a relative crossing percentage. An illustration of the ‘Kandrup Effect’ and its violation, measured by the  $\theta$  parameter, is presented in Figures 1a and 1b, for the 31 halos in order of increasing mass.

We remark that one expects that the values of energies of the particles in a clump (after the formation-collapse of it) are spread in a wider range than the range of their initial energies. During the collapse and relaxation, a number of particles in the clump loose energy and they are trapped in a deeper potential well near the center of the clump, while other particles gain energy and they may even escape the clump after the collapse. This produces a wider range of energies at the final configuration. However, in the various panels of Figs. 1a and 1b we see that the final energies are almost always distributed in a smaller range than the initial energies (with only three or four exceptions). Such a description is generally the correct expectation for energies evaluated at a fixed background. But in the present case, the energies are calculated with respect to the comoving frame.

A qualitative understanding of the results of Figures 1a and 1b is the following. First, consider two particles (1 and 2) comoving with the expansion. Then, after a given time  $t' > t_0$  (where  $t_0$  is the initial time considered), their comoving coordinates are  $x_1(t_0) = x_1(t')$ ;  $x_2(t_0) = x_2(t')$ , and their potential energy (with respect to the comoving frame) is unchanged, although they might seem drifting apart from each other for an observer at a fixed reference frame. Now consider that the two particles just detach from the expansion (‘turn-around’): even though with respect to a fixed frame their potential energy may look unchanged, it does get more negative with respect

to the comoving frame (because  $x_1(t_0) > x_1(t')$ ;  $x_2(t_0) > x_2(t')$ ). Subsequently, the particles get bound, their potential energy gets more negative in both fixed and comoving frames, but it is then clear that it gets even more negative in the latter case, because the background is expanding. The same reasoning is natural to escaping particles. Also, notice that the velocity used is the peculiar velocity, which is the velocity subtracted from the velocity of expansion. The overall result to the energy calculated this way is that the particles will present final energies almost always distributed in a smaller range than the initial energies.

Notice that Figs. 1a and 1b refer to the initial and final *mean* energies of fixed collections of particles. The particles have been initially ranked according to their energies (comoving), and binned to a fixed number of particles per ranked energy cell. The initial distribution of the energies within a given ‘mesoscopic’ energy cell is relatively uniform. However, when the halos collapse or merge, this distribution tends to get skewed towards more negative energy values. Some few particles do escape and carry energy, forming a tail in the distribution. The mean energy per cell gets more negative due to the effect explained above.

Also, in most cases of Figs. 1a and 1b, the final energies are concentrated in lower values than the initial energies, but in one case particles seem to have gained energy as they form a clump. The method used to isolate the cosmological halos is friends-of-friends, which tends to extract overdensities in a given distribution of points. We expect that several such overdensities may be considered as virialized or quasi-virialized halos, but some (few) could in fact be artifacts, one of which may be the suspect case mentioned here.

In Figure 2,  $\theta$  is plotted in terms of the mass of the identified structures in the  $z=0$  box. This Figure shows that *there is a sense in which larger and larger structures seem to evolve towards a preservation of the ‘mesoscopic’ mean energies*, whereas smaller and smaller structures tend to violate the ‘Kandrup Effect’. Intermediate-sized structures present intermediate values of  $\theta$ .

From the above trend, we infer that the dynamics of the smaller structures is probably being dominated by merging processes, whereas larger structures seem to be ruled by the collapse mechanism (intermediate-sized clusters could be collapsing structures accreting small mass systems). In order to address this question, we attempt to quantify whether it is mainly the inner radial bins of the halo which violate mean energy rank, or the outer ones.

At this point, it is important to notice that in a spherical gravitational potential,  $\Phi(r)$ , the orbit of a given particle is confined to a plane defined by its angular momentum vector,  $\vec{L}$ . The circular orbits are the ones which have the greatest  $L$  by unit mass. For a given energy per unit mass,  $E$ , among all possible  $L$ s, there will be a maximum  $L_{circ}(E)$ , which corresponds to the circular orbit (c.f. Binney & Tremaine (1988)). The curve  $L_{circ}(E)$  divides the  $[E,L]$  plane into a forbidden (above the curve) and a populated (below the curve) region, were the particles of a given gravitational system will lie. (Deviations from spherical symmetry are recognized as the presence of a few particles above the  $L_{circ}(E)$  curve in the forbidden region). It can be easily shown that the curve  $L_{circ}(E)$  tends asymptotically to  $L \rightarrow 0$  for very bound (negative) particle energies, and

$L \rightarrow \infty$  for  $E \rightarrow 0^-$ . Hence, particles with very negative energies (boundest particles) tend to have lower  $L$ , and tend to be at the inner radii of the system; on the other hand, particles less gravitationally bound tend to have a larger range of  $L$ s and mainly populate the outer radii of the system. Hence it can be reasonably assumed that the most negative energy bins analysed are composed of particles mostly at the inner radii of the halos.

Having said this, we have analysed the behaviour of the 3 innermost and 3 outermost energy bins, as explained in the following. For each halo, we have assigned a value of 1 (=YES) whenever rank violation is found within each of these two sets of 3 bins (separately), and assigned value 0 (=NO) if rank is preserved. Figure 3 illustrates the results found. It can be seen that the 3 outermost energy bins violate rank ordering in 19 out of the 31 halos, whereas for the 3 innermost bins the statistics is 29 out of 31. So, whenever rank violation occurs, it does mainly at the most bounded energy bins, which means that, for the most part, the particles at the inner radii of the model are mainly affected, not the outer ones.

### 3. Characteristic Frequencies of Collections of Particles in Dark Matter Halos

At this point, two natural questions are: first, could the phenomenon observed in Fig. 2 be artificially created solely because of the different number of particles involved in each halo? That is, could it be that, depending on the number of particles (namely, mass) of the individual halo in question, the system could artificially be more fine-partitioned relatively to a system with more particles, and hence the former system could show up more violation of the ‘Kandrup Effect’ than the latter? In fact, Kandrup et al. have analysed the problem of coarse-graining (partitioning the energy space into 5 and 20 bins) and found no significant dependence on coarse-graining. We adopt a cautionary position and identify the halos in which poor statistics may be a problem. We find that 7 out of the 31 evaluated halos have total number of particles less than 200, which implies less than 20 particles per bin. Figure 2 indicates the halos where the phenomenon (namely, rank violation as mass decreases) could be an artifact due to mass (particle) resolution. However, for the majority of halos, the number of particles per energy cell is reasonably larger than the number of coarse-grained cells adopted (10 cells, in the present case).

A second, related question is: (i) what is the coarse-graining level relevant to the observation of the ‘Kandrup Effect’, and (ii) why it happens? Concerning the latter part of the question, one of the possible explanations for the ‘Kandrup Effect’, given by Kandrup et al. themselves, but not proven, is the existence of some *constraint* operative only at the level of *collections* of particles ranked by mean energy. We try to find some clues on this problem by attempting to answer the first part of the above question. One independent method which may prove interesting is to directly verify the validity of the theorem described by Arnold (1989), concerning the behaviour of the characteristic frequencies of a dynamical system under the imposition of a linear constraint.

Arnold’s theorem describes how the characteristic frequencies ( $\omega$ ) of a system with  $n$  degrees

of freedom are distributed relatively to the characteristic frequencies ( $\omega'$ ) of a system obtained from the former under the imposition of a linear constraint, reducing the dimensionality of the given system to  $n - 1$ . The theorem goes as follows. Let

$$\omega_1 \leq \omega_2 \leq \dots \leq \omega_n \quad (3)$$

be the  $n$  characteristic frequencies of the original system where no constraints are imposed, and

$$\omega'_1 \leq \omega'_2 \leq \dots \leq \omega'_{n-1} \quad (4)$$

the  $n - 1$  characteristic frequencies of the system with a constraint. Then the theorem asserts that:

$$\omega_1 \leq \omega'_1 \leq \omega_2 \leq \omega'_2 \leq \dots \leq \omega_{n-1} \leq \omega'_{n-1} \leq \omega_n. \quad (5)$$

Let us define the characteristic frequency of a particle of the simulation as  $\omega \equiv |\vec{L}|/|R|^2$ , where  $\vec{L}$  is the angular momentum of the particle relatively to the comoving center of mass (CM) of the system and  $R$  the comoving distance of the given particle to the CM. We have taken the mean frequency values of particles grouped according to the same rank ordering method of Kandrup et al., and then proceeded as follows. We focused on the five halos that mostly violate the ‘Kandrup Effect’ and the five ones mostly obeying it. We have partitioned these halos into 9 orderly energy coarse grainings (bins) at  $z = 0$ . At  $z = 10$ , however, the 9 corresponding bins were repartitioned into 10 bins. This allowed us to directly compare the characteristic mean frequencies of each bin per halo at the two different redshifts. That is, from Eq.(4) above, the primed values now refer to the mean frequencies of each of the 9 bins analysed at  $z = 0$  (per halo), and the unprimed values, to the 10 bins at  $z = 10$  (per halo). Then, for each halo, we were able to analyse whether Arnold’s theorem (Eq. 4) would be violated or not, and at what level. We found that the percentages of halos matching Arnold’s theorem, bin by bin, for the halos mostly obeying the ‘Kandrup Effect’ (in order of decreasing mass), were: 100%, 100%, 77.8%, 66.7%, and 77.8%. For the halos violating energy rank: 33.3%, 55.5%, 66.7%, 66.7%, and 44.4%. Hence, the most massive halos tend to obey Arnold’s theorem (on the ordering of the characteristic frequencies) more frequently than less massive halos.

#### 4. Discussion

Our general conclusion is drawn from a combination of previous and present clues on the phenomenon of relaxation. Collapses are quite different from mergers, despite the fact that both are the end results of a dynamics based on fluctuations on the gravitational potential. These main differences are at the heart of the connection between the ‘Kandrup Effect’ and the  $FP \times$  virial relations.

From the current interpretation, merging of stellar systems occurs due to a transfer of the orbital energy to the particles within the systems through tidal interactions. This mechanism

increases the internal energy of the systems at the expense of their orbital energy. If the orbital energy is less negative (approaches  $0^-$ ), there is plenty of time for the particles to withdraw energy from the orbit of the pair of merging models. This process involves periodically, slowly evolving, large fluctuations on the potential, which takes a larger amount of time to stabilize. It was already evident that such slow of stabilization process could be responsible for producing non-homology among the simulated mergers (Capelato et al. 1995; Dantas et al. 2003). Collapses, on the contrary, are generally much more ‘violent’ than mergers, even those resulting from relatively ‘warm’ initial conditions.

The present analysis corroborates the idea that collapses and mergers behave differently from the point of view of their energy rank preservation/violation, considering that both mechanisms are dominant at different scaling (mass) regimes. Indeed, we find that:

- More massive halos tend to better preserve their mean energy rank ordering than less massive halos.
- Whenever rank violation occurs, it does mainly at the most bounded energy bins, which means that, for the most part, the particles at the inner radii of the model are mainly affected, not the outer ones. This is in agreement with the qualitative idea that the central region of the halo is where the gravitational potential fluctuates more strongly during the collapse, whereas in the outer regions of the halo the fluctuations are softer and dump rapidly. In the case of mergers, however, it is expected that the outer regions will be submitted to equally large fluctuations because of the anisotropy of the merging geometry as compared to a simple, isotropic collapse. Indeed it is interesting to notice that rank violation of the 3 outermost bins does occur much more frequently for less massive halos, where merging is expected to occur more frequently as well.
- The process of mesoscopic ‘mixing’ in the energy space seems to be inefficient as compared with ‘mixing’ in configuration and/or velocity space, an effect which is at odds with Lynden-Bell’s theory of complete ‘violent relaxation’ (Lynden-Bell 1967); see discussion in Kandrup et al. However, this effect seems to be more evident depending on the process of virialization (collapses seem more prone to energy rank preservation).
- We provide a general method to evaluate the coarse-graining level (number of particles per energy cell) relevant to reasonably measure signatures of the ‘Kandrup Effect’. We have observed that Arnold’s theorem, applied to the collections of particles of each energy bin, tends to be valid more frequently when the ‘Kandrup Effect’ is operative, than when it is not. This may be related to the presence of a ‘mesoscopic constraint’ operative at the level of particles, as observed by Kandrup et al. Alternatively, when Arnold’s theorem is shown not to be valid, the ‘Kandrup Effect’ is expected to be violated. In this case, one could suspect of small particle number statistics or, otherwise, intrinsic (real) energy rank violation.



We briefly assess how our results could be affected by a different choice of evaluation of energies. Kandrup et al. analysed the merging of two galaxies and have computed the energy of a given particle considering two choices:

1. relative to the common center of mass (CM) of both galaxies;
2. relative to center of mass of the galaxy in which the particle was originally located.

Kandrup et al. show that, if the initial center of mass velocity is relatively small, the tendency (preservation of the ordering of the mean ranked energies of collections of particles) is little affected (methods 1 and 2 give similar results), although the effect does get weaker if the velocity of the CM is reasonably large. Notice however that the simulations of Kandrup et al. were performed on a fixed background. In the present situation the energies are all comoving quantities, the velocity of expansion of the cosmological background does not enter into the above computations, so it is our opinion that our choice of evaluation of energies is reasonable in the cosmological set. A posteriori, our results (Fig.1a and 1b) do reproduce the ‘Kandrup Effect’.

We also consider the question whether our results depend on the position of the particular clump inside the simulation box. A qualitative reasoning indicates that they must not, since we calculate the comoving energies with no reference to the relative location within the simulation box. Also, the halos analysed in the paper are distributed at several locations within the simulation box, and the results are reasonably similar among them, irrespective of their position, depending mostly on the halo mass.

We would like to draw attention to the relation of our results to those of the recent paper by Hansen et al. (2005). These authors have studied the velocity distribution function (VDF) of different gravitational systems (from isotropic to highly non-isotropic structures), simulated from diverse N-body experiments, including cosmological ones, and found that the VDF has a universal profile. This may indicate that some fraction of the particles of a gravitational system exchange energy during the relaxation process only until the universal VDF has been reached. It would be highly interesting to understand the relation between energy rank preservation and the universal VDF.

In summary, the scenario presented here, although admittedly schematic, does offer some preliminary important clues on the origin of the scaling relations of virialized systems. However, a rigorous understanding of the relaxation process still lacking (Padmanabhan 1990), in order to reach a complete understanding of the phenomena outlined in this paper.

## Acknowledgements

The simulations in this paper were carried out by the Virgo Supercomputing Consortium using computers based at Computing Centre of the Max-Planck Society in Garching and at the Edinburgh Parallel Computing Centre. The data are publicly available at [www.mpa-garching.mpg.de/NumCos](http://www.mpa-garching.mpg.de/NumCos). We thank Dr. André L. B. Ribeiro for several discussions, and the anonymous referee for useful suggestions. C.C.D. thanks Instituto Nacional de Pesquisas Espaciais (INPE), Divisão de Astrofísica (DAS/CEA), Brazil, for using its facilities when most part of this paper was written.

## REFERENCES

- Arnold, V. I., *Mathematical Methods of Classical Mechanics*, 2nd. edition, 1989, Springer-Verlag, New York.
- Bekki, K., 1998, ApJ, 496, 713.
- Binney & Tremaine, *Galactic Dynamics*, Princeton University Press.
- Capelato, H. V., de Carvalho, R. R. & Carlberg, R. G., 1995, ApJ, 451, 525.
- Dantas, C. C., Ribeiro, A. L. B., Capelato, H. V., and de Carvalho, R. R., 2000, ApJ, 528, L5.
- Dantas, C. C., Capelato, H. V., de Carvalho, R. R., & Ribeiro, A. L. B., 2002, A&A, 384, 772.
- Dantas, C. C., Capelato, H. V., Ribeiro, A. L. B. & de Carvalho, R. R., 2003, MNRAS, 340, 398.
- Dantas, C. C. & Ramos, F. M., 2005, ApJ, submitted.
- Djorgovski, S. G. & Davis, M., ApJ, 1987, 313, 59.
- Djorgovski, S. G., in Proc. Moriond Astrophysics Workshop, 1988, Starbursts and Galaxy Evolution, ed. T. X. Thuan et al. (Gif sur Yvette: Editions Frontières), 549.
- Djorgovski, S. G., in Cosmology and Large-Scale Structure in the Universe, ASP Conference Series, Vo. 24, 1992, Reinaldo R. de Carvalho, (ed.), 19.
- Djorgovski, S. G. & Santiago, B. X., 1993, in *Structure, Dynamics and Chemical Evolution of Elliptical Galaxies*, Proc. ESO/EIPC Workshop, ed. I. J. Danziger, W. W. Zeilinger, & K. Kjar (ESO Conf. and Workshop Proc. 45) (Garching:ESO), 59
- Dressler, A., Lynden-Bell, D., Burstein, D., Davies, R. L., Faber, S. M., Terlevich, R. J., & Wegner, G., 1987, ApJ, 313, 42.
- FOF Algorithm, <http://www-hpcc.astro.washington.edu/tools/fof.html>.
- Hansen, S. H. et al., astro-ph/0505420

- Hjorth, J. & Madsen, J., 1995, ApJ 445, 55.
- Kadrop, H. E., Mahon, M. E., & Smith, H., 1993, A&A 271, 440.
- Longair, M., Galaxy Formation, Springer, page 366.
- Lynden-Bell, D., 1967, MNRAS 136 101.
- May & van Albada, 1984, MNRAS, 209, 15
- Padmanabhan, T., 1990, Physics Reports, 188, No.5, 285-362.
- Pahre, M., 1998, PhD Thesis, California Institute of Technology.
- Quinn & Zurek, 1988, ApJ, 331 ,1
- van Albada 1982, MNRAS, 201, 939
- Voglis, Hiotelis & Hoefflich, 1991, A& A, 249, 5
- Voglis, Hiotelis & Harsoula, 1994, Astrophysics and Space Science, 226, 213.
- Zaroubi et al., 1996, ApJ, 457, 50
- White, S., 1979, MNRAS, 189, 831

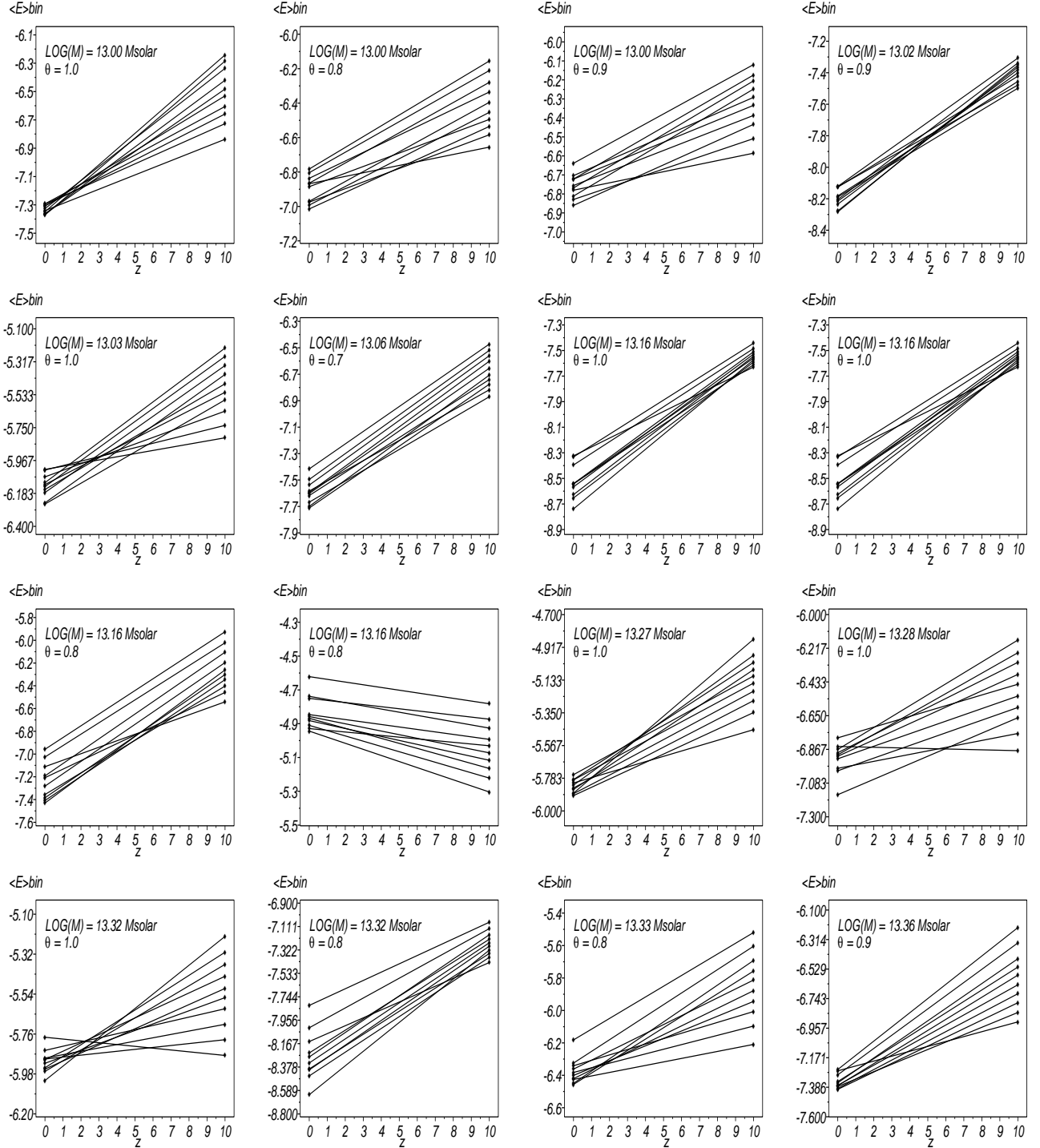


Fig. 1.— (a) The ‘mesoscopic’ mean energy of fixed number of particles ( $\langle E \rangle_{bin}$ ) at  $z = 0$  (final condition) and  $z = 10$  (initial condition), connected by line segments in order to illustrate the ordering of the mean energy of given collections of particles, from the most gravitationally bounded ones (most negative energies) to the less bounded ones (less negative energies). The panels are ordered from the less massive halos (top left panel) to the most massive halos (bottom right panel). The second panel (from left to right) at the third row is possibly an overdensity artifact (not a virialized halo).

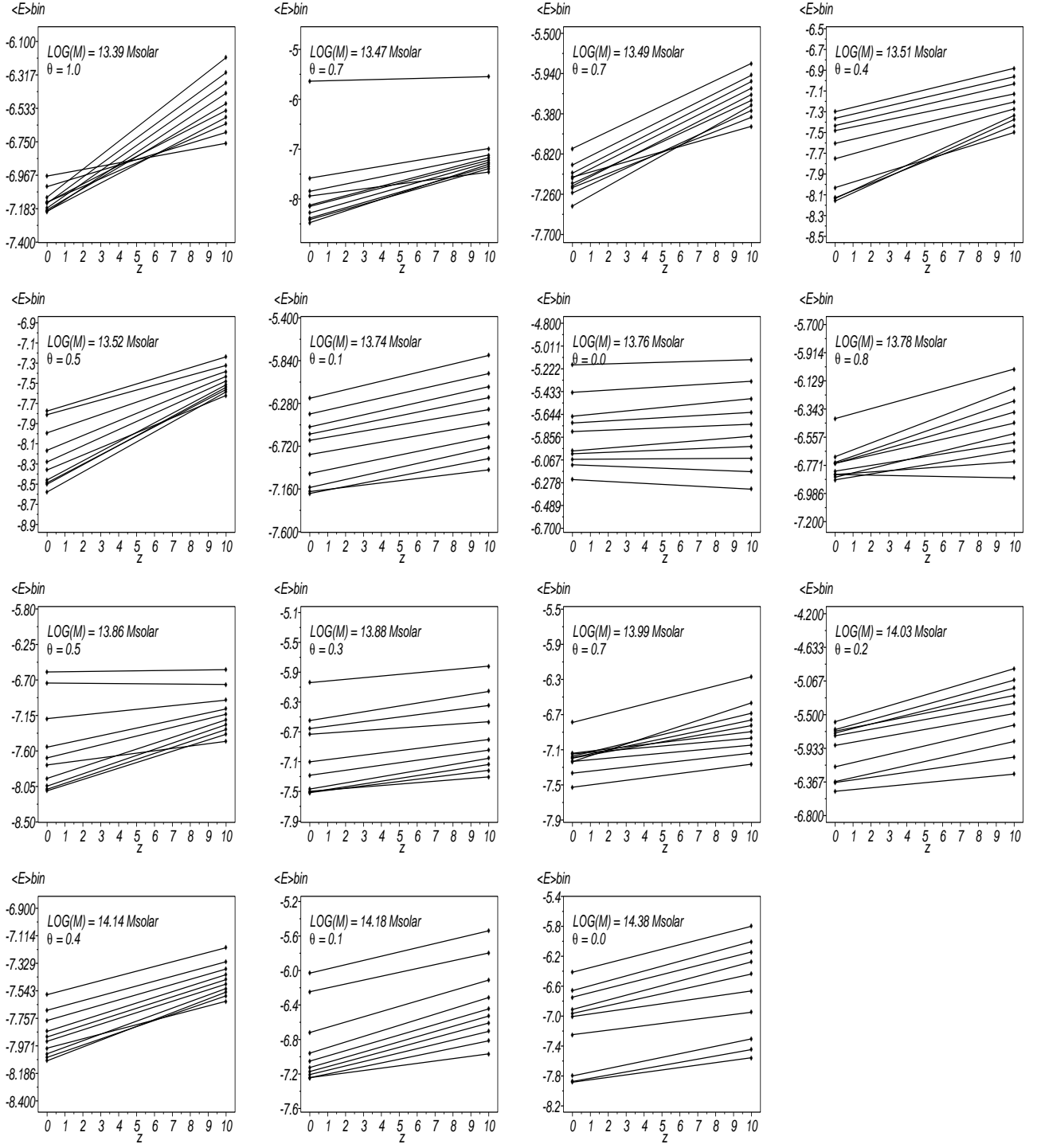


Fig. 1.— (b) Continued from Fig. 1a.

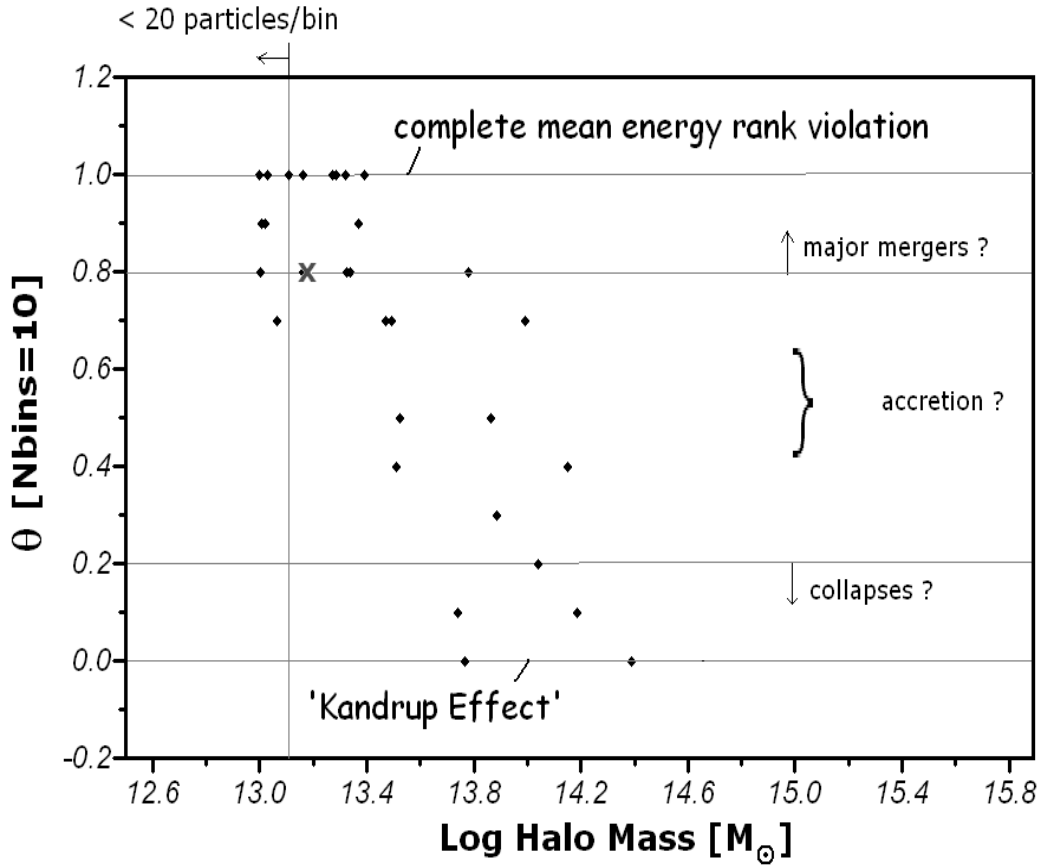


Fig. 2.— The ‘mesoscopic’ mean energy ordering violation rate ( $\theta$ ) as a function of the halo mass in a  $z=0$   $\Lambda$ -CDM cosmological box. Possible dynamical events are identified in this figure. The object marked with an ‘X’ is possibly an overdensity artifact (not a virialized halo).

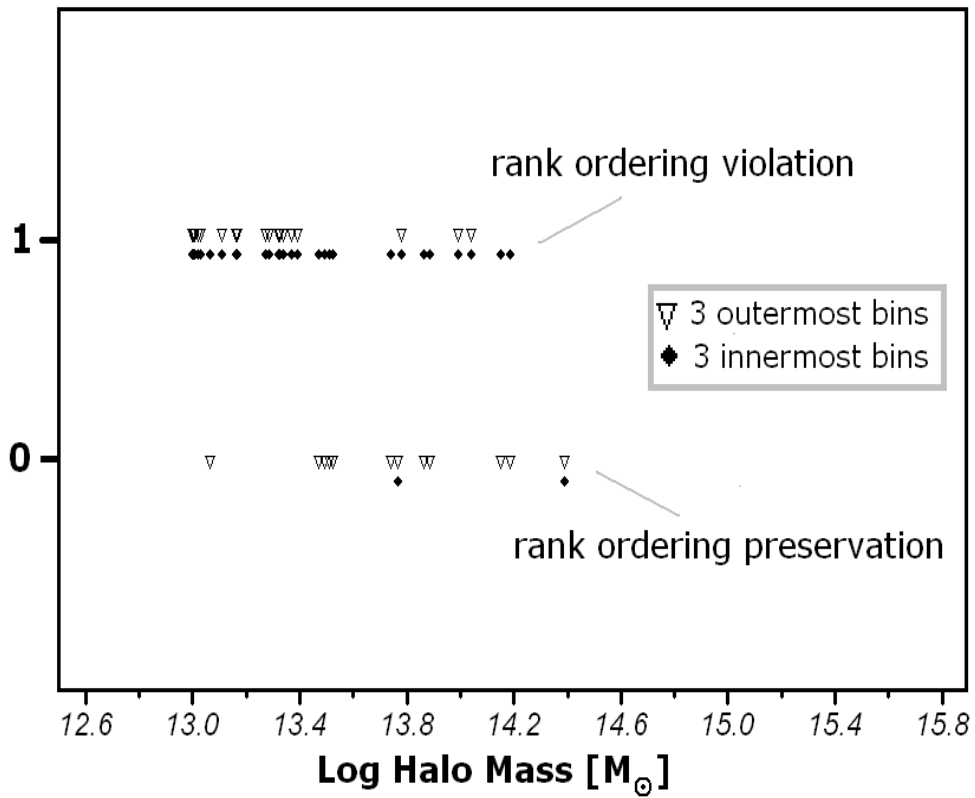


Fig. 3.— Analysis of the 3 innermost and 3 outermost energy bins of all 31 halos considered. Violation (preservation) of energy rank is signaled at the vertical axis by the value 1 (0).